Supporting Information

Synthesis of Bifunctional Ru-Pd Catalysts Following the Double Reduction Method: Hydrogenation/Dehydrogenation of Liquid Organic Hydrogen Carriers

Ting Zhu [a], Ran Wang [a], Ziteng Chen[a], Feng Ji[b], Yuan Dong[a], Ming Yang [a, c] *

[a] *Sustainable Energy Laboratory, Faculty of Materials Science and Chemistry, China University of Geosciences, Wuhan 430074, China*

[b] *State Key Laboratory of Space Power-Sources Technology, Shanghai Institute of Space Power Sources, Shanghai 200245, China*

[c] *Zhejiang Institute, China University of Geosciences, Hangzhou, 311305, China*

**Corresponding authors. E-mail address: yangming8180@gmail.com (Ming Yang).*

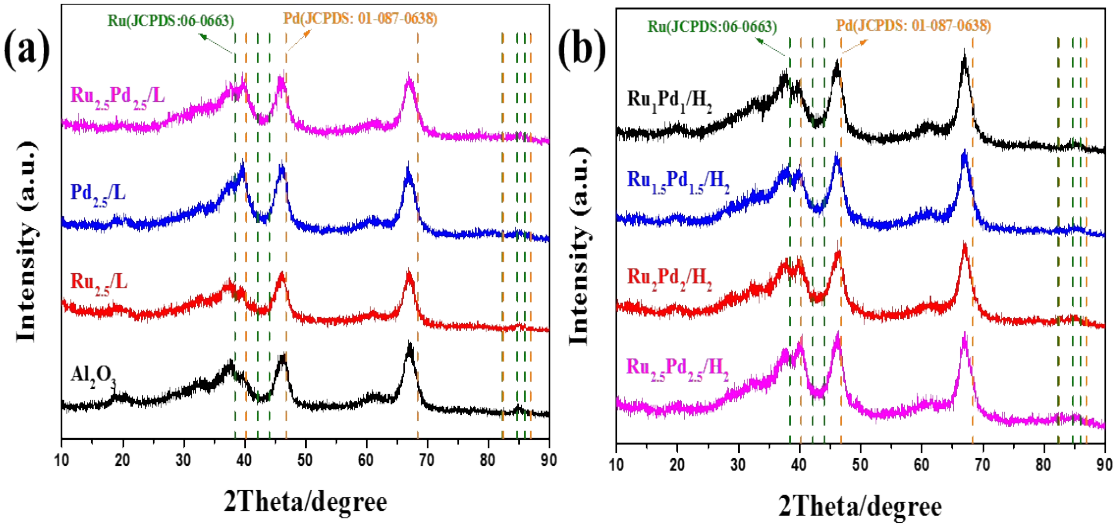

Fig. S1. (a) XRD plots recorded for the $Ru_{2.5}$/L, $Pd_{2.5}$/L and $Ru_{2.5}Pd_{2.5}$/L catalysts prepared following the liquid-phase reduction method; (b) XRD plots recorded for the $Ru_{2.5}Pd_{2.5}/H_2$, Ru_2Pd_2/H_2, $Ru_{1.5}Pd_{1.5}/H_2$, and Ru_1Pd_1/H_2 catalysts prepared following the double reduction method.

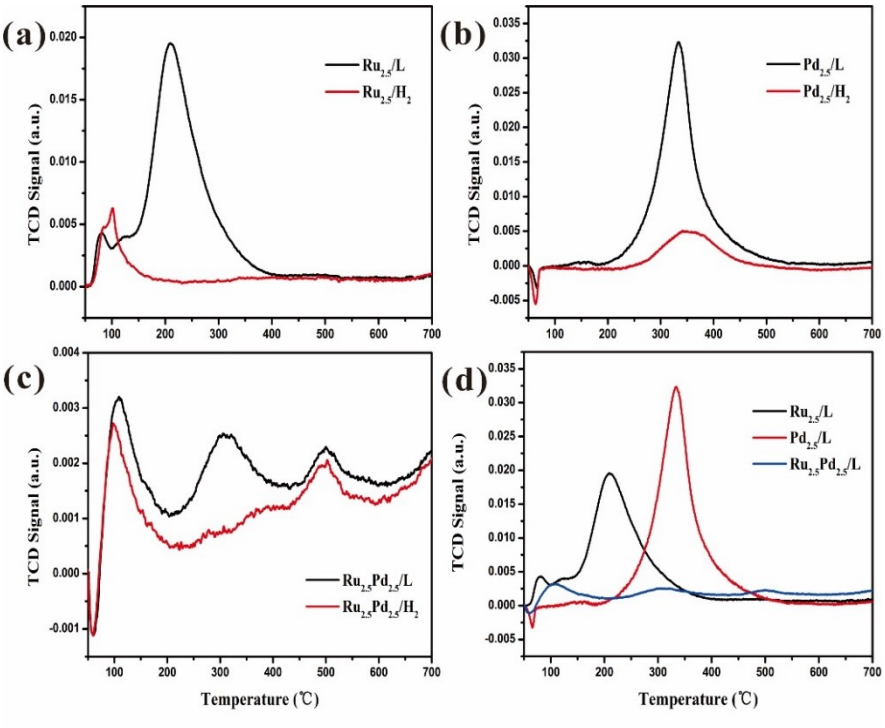

Fig. S2. H_2-TPR-based comparison of catalysts prepared following the liquid-phase reduction ($Ru_{2.5}$/L, $Pd_{2.5}$/L, $Ru_{2.5}Pd_{2.5}$/L) and double reduction methods ($Ru_{2.5}/H_2$, $Pd_{2.5}/H_2$, $Ru_{2.5}Pd_{2.5}/H_2$).

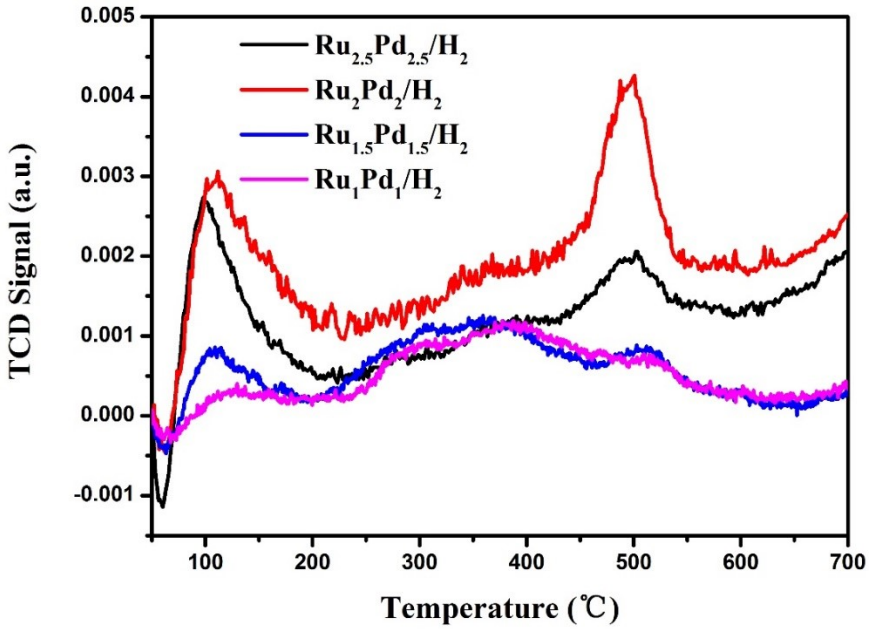

Fig. S3. H_2-TPR plots recorded for the $Ru_{2.5}Pd_{2.5}/H_2$, Ru_2Pd_2/H_2, $Ru_{1.5}Pd_{1.5}/H_2$, and Ru_1Pd_1/H_2 catalysts prepared following the double reduction method.

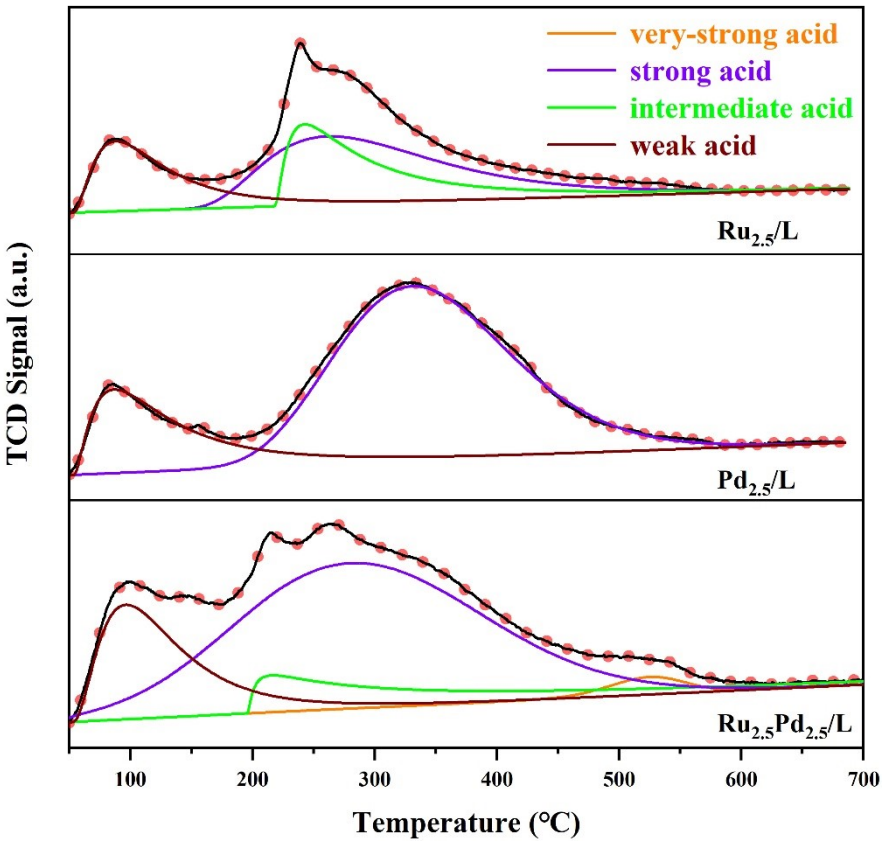

Fig. S4. NH_3-TPD plots recorded for the $Ru_{2.5}$/L, $Pd_{2.5}$/L and $Ru_{2.5}$ $Pd_{2.5}$/L catalysts prepared following the liquid-phase reduction method.

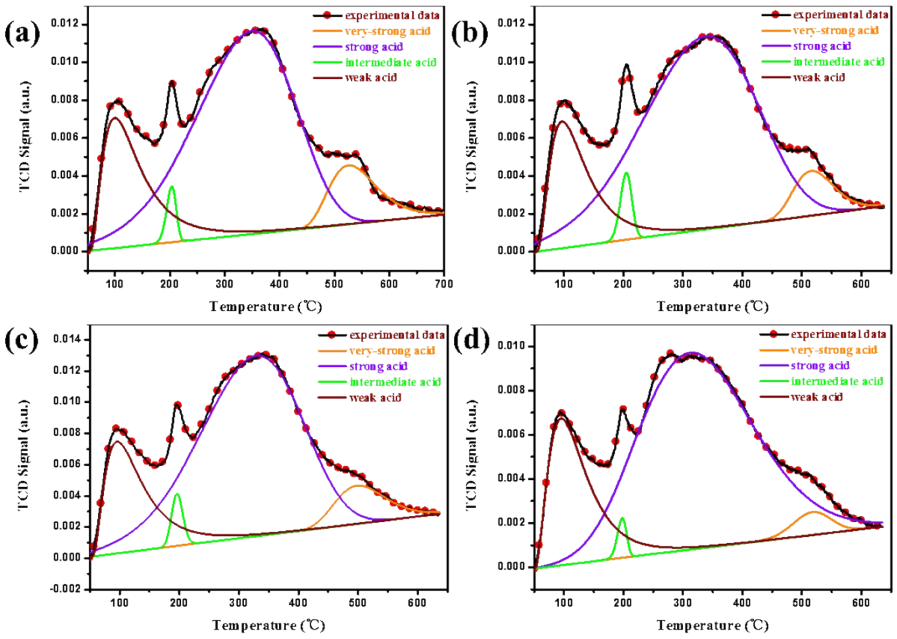

Fig. S5. NH_3-TPD plots recorded for the $Ru_{2.5}Pd_{2.5}/H_2$, Ru_2Pd_2/H_2, $Ru_{1.5}Pd_{1.5}/H_2$, and Ru_1Pd_1/H_2 catalysts prepared following the double reduction method.

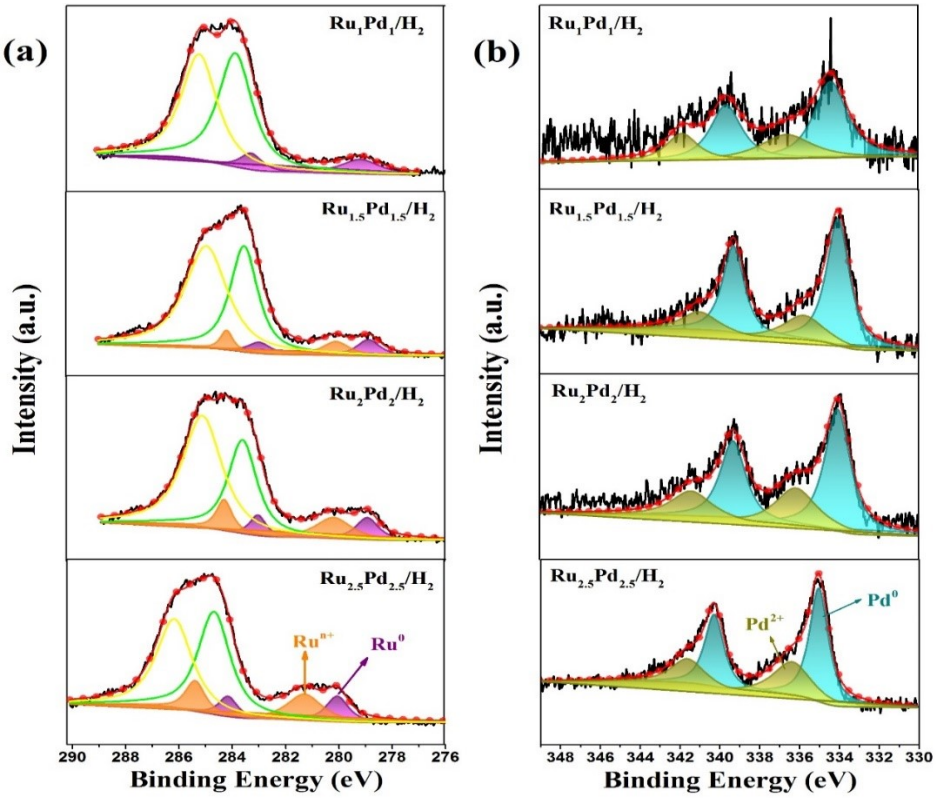

Fig. S6. (a) Plot of the Ru 3d core level fitting peaks obtained using the XPS technique for the $Ru_{2.5}Pd_{2.5}/H_2$, Ru_2Pd_2/H_2, $Ru_{1.5}Pd_{1.5}/H_2$, and Ru_1Pd_1/H_2; (b) Plot of the Pd 3d core level fitting peaks obtained using the XPS technique for $Ru_{2.5}Pd_{2.5}/H_2$, Ru_2Pd_2/H_2, $Ru_{1.5}Pd_{1.5}/H_2$, and Ru_1Pd_1/H_2.

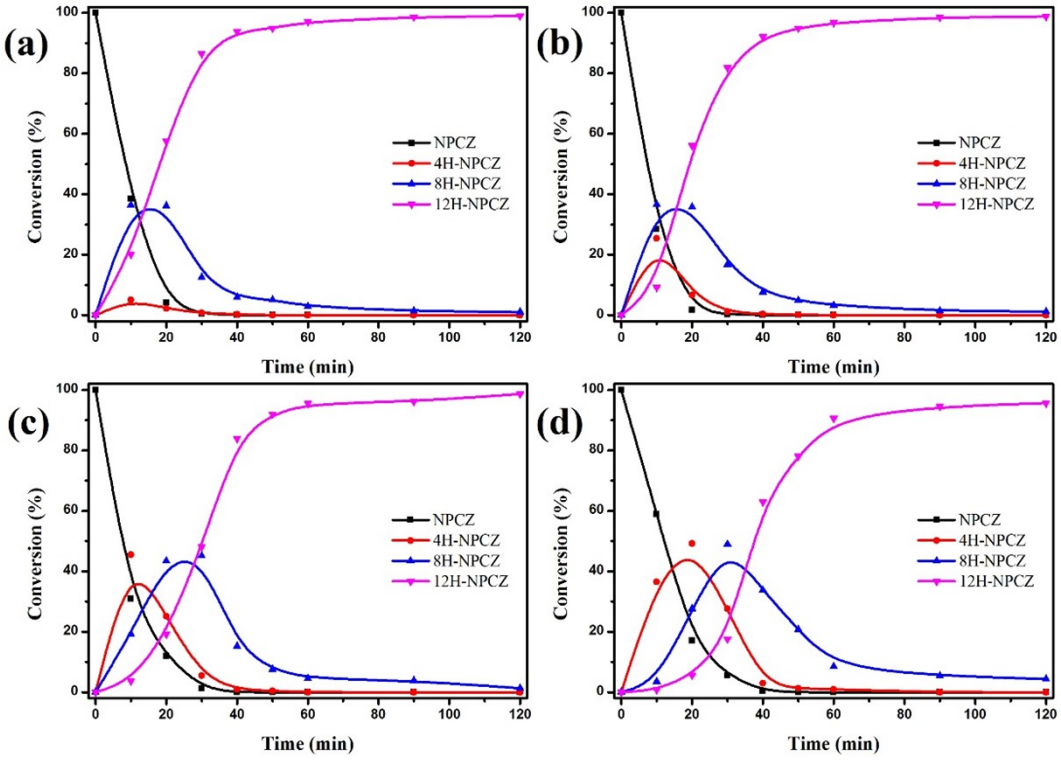

Fig. S7. Time-dependent product distribution recorded for NPCZ hydrogenation with different catalysts: (a) $Ru_{2.5}Pd_{2.5}/H_2$, (b) Ru_2Pd_2/H_2, (c) $Ru_{1.5}Pd_{1.5}/H_2$, and (d) Ru_1Pd_1/H_2.

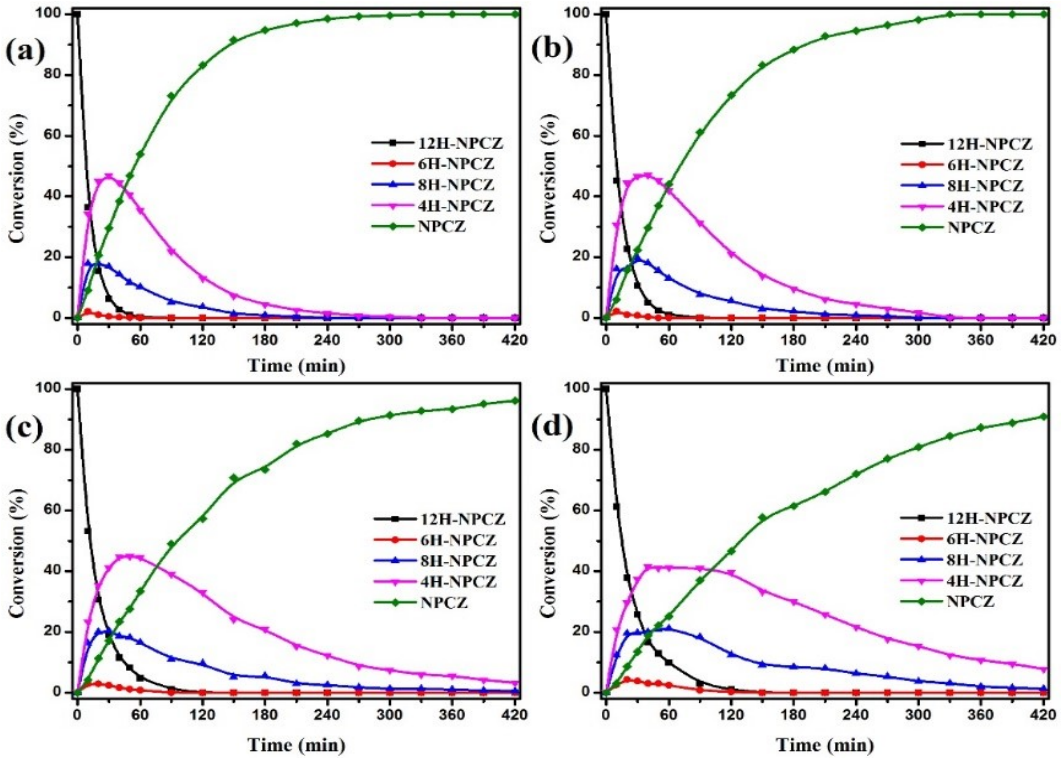

Fig. S8. Time-dependent product distribution recorded for 12H-NPCZ dehydrogenation with different catalysts: (a) $Ru_{2.5}Pd_{2.5}/H_2$, (b) Ru_2Pd_2/H_2, (c) $Ru_{1.5}Pd_{1.5}/H_2$, and (d) Ru_1Pd_1/H_2.

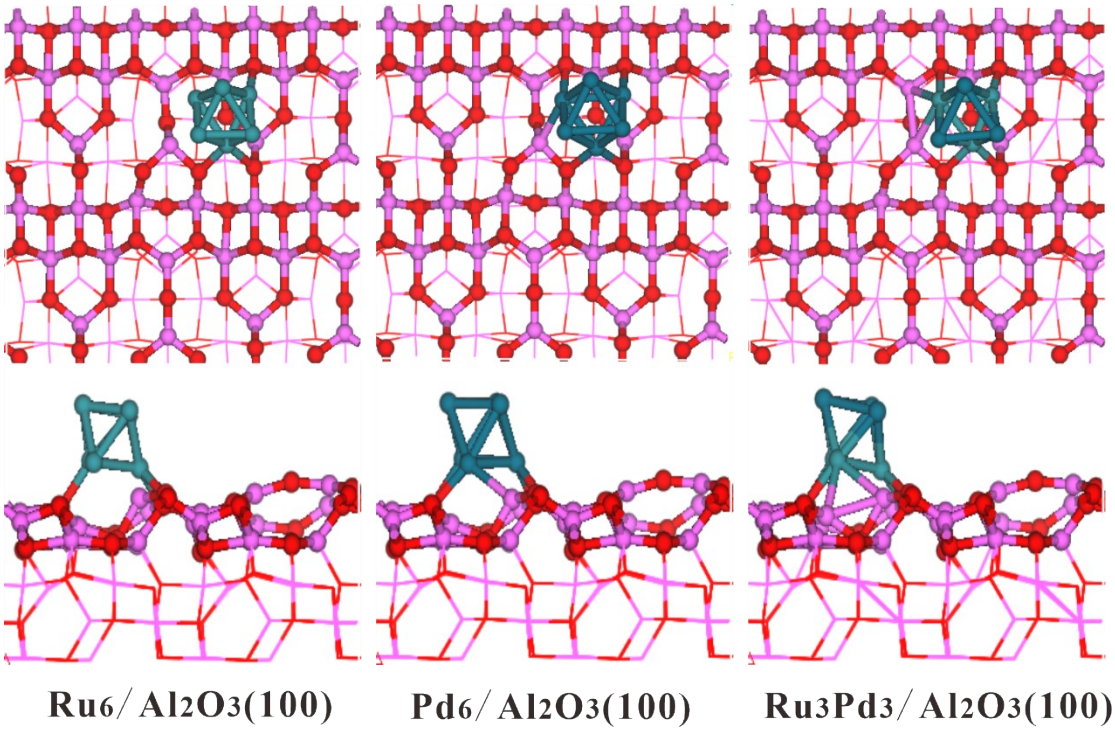

Fig. S9. Top and side view of the configurations of $Ru_6/Al_2O_3(100)$, $Pd_6/Al_2O_3(100)$, and $Ru_3Pd_3/Al_2O_3(100)$; dark green, light green, pink and red balls represent the Pd, Ru, Al and O atoms, respectively.

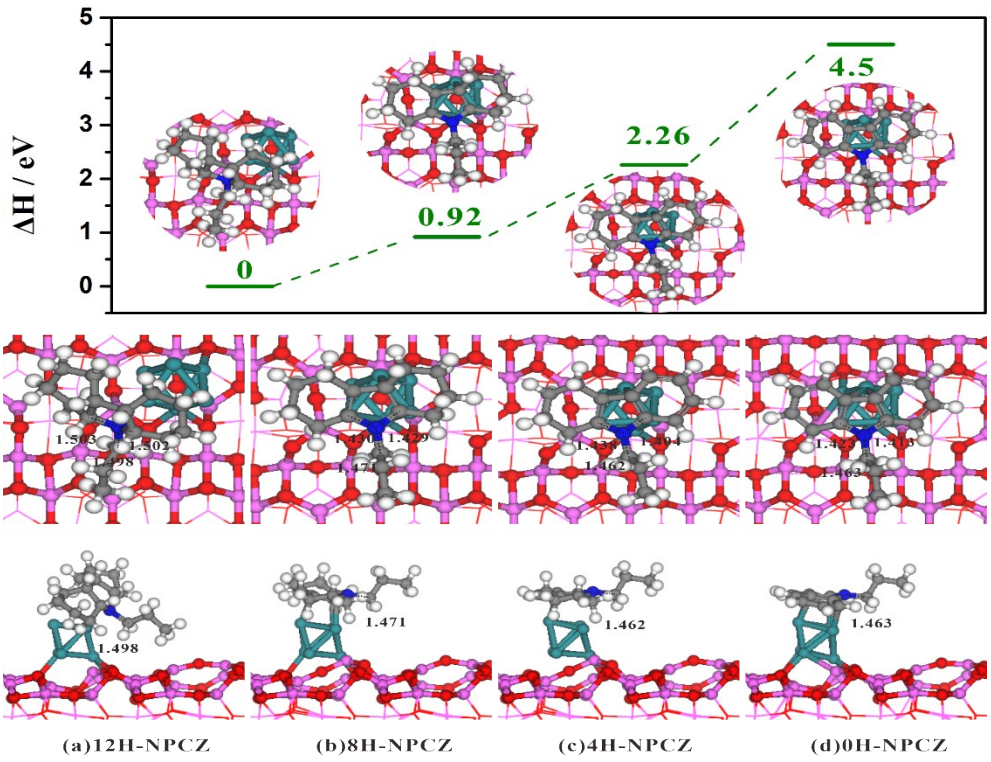

Fig. S10. Energy profile from 12H-NPCZ→8H-NPCZ→4H-NPCZ→NPCZ on $Ru_6/Al_2O_3(100)$ surface; light green, pink, red, white and blue balls represent the Ru, Al, O, H, and N atoms, respectively.

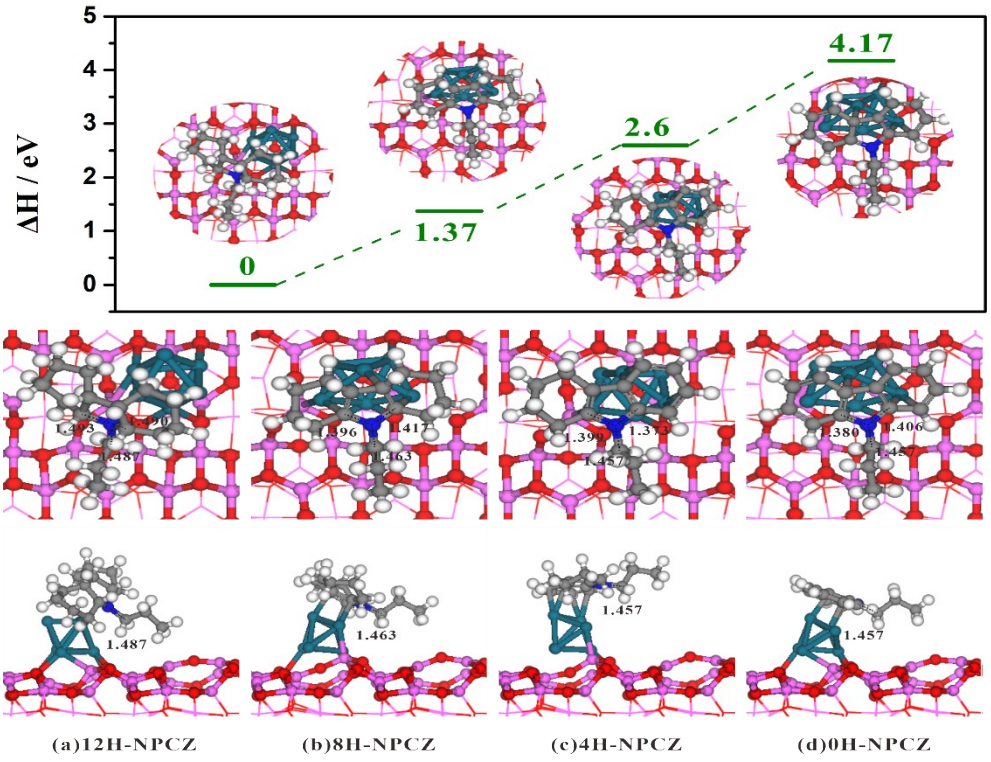

Fig. S11. Energy profile recorded for 12H-NPCZ→8H-NPCZ→4H-NPCZ→NPCZ on $Pd_6/Al_2O_3(100)$ surface; dark green, pink, red, white, and blue balls represent the Pd, Al, O, H, and N atoms, respectively.

Table S1. Acid characteristic of catalysts in this article.

	Acidity [μmol·g^{-1}][a]					Acid site density [site nm^{-2}][d]			
	Total[b]	**Wea[c]**	**Int[c]**	**Str[c]**	**V-str[c]**	**Wea[d]**	**Int[d]**	**Str[d]**	**V-str[d]**
$Ru_{2.5}$/L	942.37	220.04 88 °C	280.95 242 °C	441.38 261 °C	—	0.74	0.94	1.48	—
$Pd_{2.5}$/L	1128.69	244.01 86 °C	—	884.68 330 °C	—	0.75	—	2.70	—
$Ru_{2.5}Pd_{2.5}$/L	1154.70	233.96 96 °C	131.43 215 °C	758.98 280 °C	30.33 524 °C	0.55	0.31	1.78	0.07
$Ru_{2.5}Pd_{2.5}/H_2$	974.94	193.84 99 °C	20.06 203 °C	663.64 349 °C	97.40 525 °C	0.54	0.056	1.84	0.27
Ru_2Pd_2/H_2	919.86	165.79 96 °C	26.12 204 °C	670.52 338 °C	57.43 515 °C	0.52	0.082	2.10	0.18
$Ru_{1.5}Pd_{1.5}/H_2$	844.40	162.31 95 °C	21.41 196 °C	595.44 329 °C	65.24 498 °C	0.50	0.067	1.85	0.20
Ru_1Pd_1/H_2	833.80	177.93 95 °C	12.43 197 °C	617.62 311 °C	25.82 517 °C	0.46	0.032	1.60	0.07

[a] [b] [c] The value of acidity obtained by NH3-TPD quantification experiments.

[c] The value in brackets represents the temperature at the center of ammonia desorption peak.

[d] Surface density of the acid site.

Table S2. Bind energy of Ru3d and Pd3d core-level obtained by XPS experiments.

	Binging Energy (eV)				Contribution	Contribution
	Ru^0 $3d_{5/2}$	Ru^{n+} $3d_{5/2}$	Pd^0 $3d_{5/2}$	Pd^{2+} $3d_{5/2}$	of Pd^0 (%)	of Ru^0 (%)
$Ru_{2.5}Pd_{2.5}/H_2$	280.07	281.30	335.04	336.38	63.68	38.55
Ru_2Pd_2/H_2	278.91	280.18	334.05	336.16	67.05	39.95
$Ru_{1.5}Pd_{1.5}/H_2$	278.86	280.08	334.03	335.75	74.79	50.41
Ru_1Pd_1/H_2	279.18	—	334.38	336.59	65.10	100

Table S3. Selectivity of reaction species of NPCZ to 12H-NPCZ and H_2-uptake amount over different catalysts in 30 min at 150 °C and pressure of 7 MPa H_2.

Catalysts	Conversion %	Selection %			H_2-Uptake
	NPCZ	4H-NPCZ	8H-NPCZ	12H-NPCZ	wt%
$Ru_{2.5}/L$	81.285	16.741	44.565	19.979	3.04
$Ru_{2.5}/H_2$	85.241	13.976	43.247	28.018	3.38
$Ru_{2.5}Pd_{2.5}/L$	100	0	7.469	92.531	5.30
$Ru_{2.5}Pd_{2.5}/H_2$	99.621	0.69	12.477	86.454	5.17
Ru_2Pd_2/H_2	99.696	1.075	16.709	81.912	5.08
$Ru_{1.5}Pd_{1.5}/H_2$	98.702	5.486	45.095	48.121	4.38
Ru_1Pd_1/H_2	94.526	27.615	48.948	17.963	3.30

Table S4. Selectivity of reaction species of 12H-NPCZ to NPCZ and H_2-release amount over different catalysts in 60 min at 190 °C.

Catalysts	Conversion %	Selection %				H_2-Release
	12H-NPCZ	8H-NPCZ	6H-NPCZ	4H-NPCZ	NPCZ	wt%
$Pd_{2.5}/L$	99.770	4.102	0	53.758	41.910	4.26
$Pd_{2.5}/H_2$	100	1.901	0	44.222	53.877	4.53
$Ru_{2.5}Pd_{2.5}/L$	94.483	12.003	1.528	42.003	39.309	3.86
$Ru_{2.5}Pd_{2.5}/H_2$	99.731	10.278	0	35.5	53.953	4.37
Ru_2Pd_2/H_2	98.974	13.069	0	41.888	44.017	4.11
$Ru_{1.5}Pd_{1.5}/H_2$	95.299	16.466	0.778	44.634	33.421	3.71
Ru_1Pd_1/H_2	90.066	21.160	2.474	41.258	25.174	3.23

Table S5. Key structural parameters and adsorption energy (E_{ads}, eV) of 12H-NPCZ, 8H-NPCZ, 4H-NPCZ, and NPCZ on the $Ru_6/Al_2O_3(100)$, $Pd_6/Al_2O_3(100)$, and $Ru_3Pd_3/Al_2O_3(100)$ surfaces.

Surfaces	Species	Adsorption/configuration	E_{ads}	C-N Bonding length (Å)		
			(eV)	C3-N	C13-N	C4-N
(a) $Ru_6/Al_2O_3(100)$	12H-NPCZ	Ru_3	-0.32	1.503	1.498	1.502
	8H-NPCZ	T_{Ru}: via C	-1.01	1.430	1.471	1.429
	4H-NPCZ	T_{Ru}: via C	-1.22	1.438	1.462	1.404
	NPCZ	T_{Ru}: via C	-0.73	1.423	1.463	1.413
(b)$Ru_3Pd_3/Al_2O_3(100)$	12H-NPCZ	T_{Ru}: via N	-1.37	1.500	1.499	1.496
	8H-NPCZ	T_{Ru}: via C	-1.23	1.424	1.466	1.447
	4H-NPCZ	T_{Ru}: via C	-1.36	1.456	1.463	1.366
	NPCZ	T_{Ru}: via C	-1.33	1.419	1.463	1.418
(c) $Pd_6/Al_2O_3(100)$	12H-NPCZ	Pd3	-0.95	1.503	1.498	1.502
	8H-NPCZ	T_{Ru}: via C	-0.12	1.430	1.471	1.429
	4H-NPCZ	T_{Ru}: via C	-1.09	1.438	1.462	1.404
	NPCZ	T_{Ru}: via C	-0.48	1.423	1.463	1.413